Evolution of PHA Response in the HRC

J. Posson-Brown, R. H. Donnelly

23rd May 2003

1 Introduction

Since launch, observations of AR Lac have been taken regularly with the HRC-I and HRC-S at multiple locations on each detector to monitor the performance of the instruments. Analyzing these observations by comparing the median source pulse-height amplitudes (PHAs) over the past few years, we find that both detectors suffer from gain loss, which is more dramatic in the case of the HRC-I than for the HRC-S. To explore a possible energy dependence in the HRC-I's gain evolution, we examined observations of HZ 43 taken over the past few years at the nominal aimpoint. We find that the gain loss in the HRC-I is also witnessed by HZ 43.

2 Analysis

For both detectors, we analyzed the level 1 event lists filtered on the nominal good time intervals (GTIs) provided in the standard filter files.[1] The level 1 event lists were selected to avoid changes in the data due to revisions of the standard pipeline processing over the years.[2]

We extracted PHAs of events within a small circular region around each source. The sizes of the regions were chosen to be small enough to exclude any significant background contribution while enclosing over 95% of the source counts.[3] Details about the sizes of the regions, as well as the position of the source on the detector for each observation, can be found in Appendix A.

For both detectors, we calculated the median source PHA for each observation after rejecting events from the highest channel (255), since this channel is often contaminated by a second peak. This second peak, particularly prominent in HRC-I observations, seems to consist of source events that are not well-understood, and is currently under investigation. We decided to treat our data

[1] The HRC-I Oct 99 data required additional time filtering; see details in Section 3.1.

[2] See *http://cxc.harvard.edu/proc_stat/rel_notes/* for release notes detailing pipeline changes.

[3] We also tested larger regions (with radii ranging from 100 - 400 pixels) designed to enclose $\sim$100% of the source counts for each position on the detector, though allowing for a potentially larger background contribution. We find that the region size affects the median PHA for any given observation by at most one channel.

as a typical user would and exclude channel 255 events. Examining how rejecting these events affects the median reveals that the effect is negligible, changing the median by at most a few channels. Since our analysis is comparative - we are interested in the median's evolution rather than the particular value for a given observation - the decision to exclude channel 255 events does not affect our results in any significant way.

For observations at the nominal aimpoint, we also estimated the average rates of change with time of the median PHA and the width of the distribution (as measured by the standard deviation of the median) by doing linear least-squares fits to the data. Finally, we fit Gaussians to the PHA distributions for observations taken at the aimpoint for both detectors to show qualitatively how the distributions are evolving. Note that the parameters from the Gaussian fits were not used in our quantitative analysis.

3 Results

3.1 HRC-I

Five sets of AR Lac observations taken with the HRC-I were considered in this analysis. The first set was taken in October 1999 in conjunction with the initial voltage adjustment done shortly after launch. Due to the specifics of the command sequence for the voltage adjustment, the beginning of each observation in this set was at the original higher voltage. So, in addition to filtering these event lists on the GTIs, we filtered them on time intervals, provided by Mike Juda, during which the voltage was at the current setting.

A second set of AR Lac observations was done in December 1999 as follow-up to the amplifier scale-factor adjustment. The remaining three sets were done as part of the standard HRC-I annual calibration observations in December 2000, January 2002, and February 2003. Each set consists of an observation at the nominal aimpoint and twenty additional observations at various offsets around the detector (listed in Table 1, Appendix A). The exposure time for each observation was approximately one kilosecond.

For all 21 monitored positions on the detector, we find that the median PHA has dropped from Oct 1999 to February 2003. This drop is most dramatic at the aimpoint (not surprising since this area receives the most photons) at about 19%. For the twenty offset positions monitored, the drop ranges from roughly 9% to 4%, decreasing with radial distance from the aimpoint. This is summarized in Figure 1. The data are ordered along the x-axis by radial distance from the nominal aimpoint. Within each set at a given distance, they are arranged in counter-clockwise order by their position in the Y-Z plane of the detector, starting at the positive Y-axis.

The changes in the PHA profiles at the aimpoint are shown qualitatively by the Gaussian fits in Figure 2. The Gaussians have been normalized by the total counts in each extracting area to facilitate easy comparison. Note that not only is the median declining with time, but the distributions are becoming narrower.

Figure 1: HRC-I AR Lac Observations: Median Source PHA

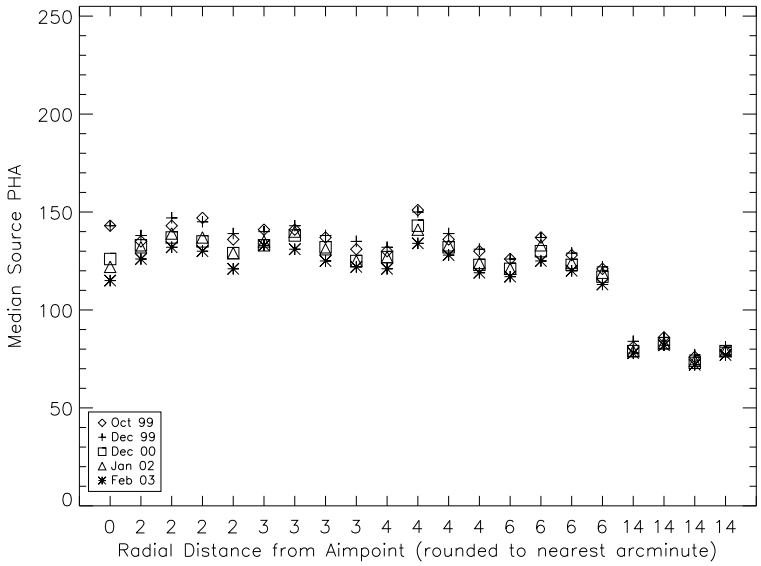

Figure 2: HRC-I AR Lac Observations: Gaussian Fits to PHA Distributions at Aimpoint

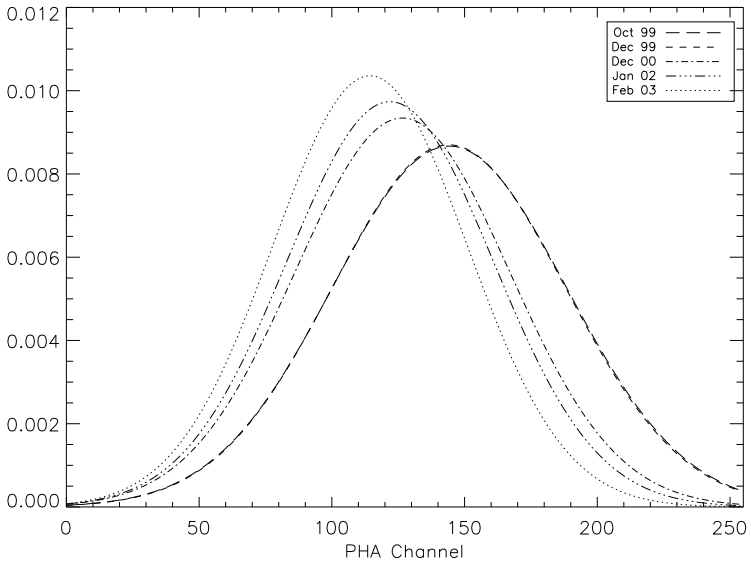

Figure 3: HRC-I HZ 43 Observations: Gaussian Fits to PHA Distributions at Aimpoint

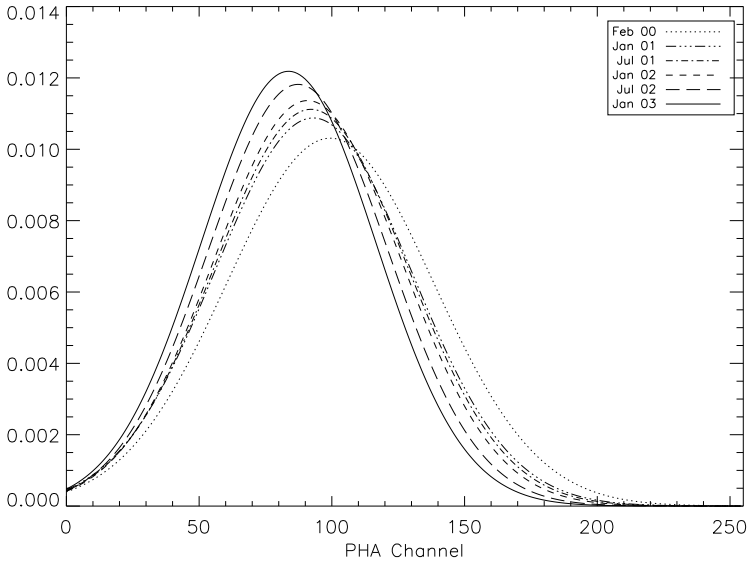

To explore if the gain loss is energy dependent, we compared the median source PHAs for six observations of HZ 43[4] taken at the nominal aimpoint over the past few years. We detect emission from HZ 43 primarily in the range of 0.06 to 0.20 keV, while emission from AR Lac peaks around 1 keV. The HZ 43 analysis was done in an identical manner to the analysis of the AR Lac observations at the aimpoint (i.e. circular extraction regions with 60 pixel radii were used and events in channel 255 were rejected). We find that the median PHA has dropped by approximately 16% and that the PHA distributions are also becoming narrower. These trends are displayed in Figures 3, which shows Gaussian fits to the PHA profiles, normalized by total counts.

Figure 4 shows the median source PHAs from the HZ 43 observations and the AR Lac observations at the aimpoint as a function of time. The solid lines are projections of the earliest value in each data set, representing trajectories without gain fatigue. Thus, deviations from these horizontal lines indicate gain evolution. The gain loss as witnessed by HZ 43 seems linear with time (dot-dash line), whereas the AR Lac medians are not well-fit by a line. Two linear least-squares fits to the AR Lac data are shown. The dashed line excludes the first two points, and is parallel to the HZ 43 linear fit, while the dotted line includes all points and gives a much steeper rate of decline. We use this steeper slope - the "worst-case scenario" - to approximate when the gain fatigue will have a non-

[4]Obs IDs 1514 (Feb 00), 1000 (Jan 01), 1001 (Jul 01), 2600 (Jan 02), 2602 (Jul 02), and 3714 (Jan 03).

Figure 4: HRC-I AR Lac and HZ 43 Observations at Aimpoint

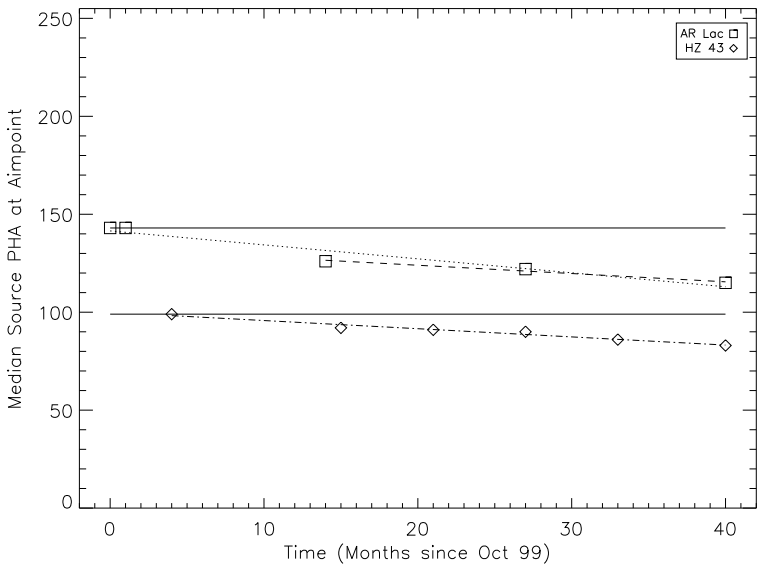

trivial impact on the detector's quantum efficiency. (We define a "non-trivial impact" as 5% of source events falling below the Lower Level Discriminator.) We estimate that it will be approximately 5 years until this occurs.

Several options are being considered to address the gain loss, one of which is to adjust the HRC-I's voltage.

3.2 HRC-S

The five sets of AR Lac observations used for the HRC-S analysis were done in December 2000, May 2001, January 2002, August 2002, and February 2003 as part of the standard calibration observations. Each set consists of one observation at the nominal aimpoint and twenty observations at various locations around the detector. (For exact positions, see Table 2 in Appendix A). As with the HRC-I, each observation was approximately one kilosecond long.

Looking at the median PHAs, we find a gain droop of about 10% or less, which is fairly uniform across the detector (see Figure 5). Examining the PHA profiles of the observations done at the nominal aimpoint, we find a slight trend of downward migration of the median and narrowing of the distribution, though it is less pronounced here than in the HRC-I. (See Figure 6, which shows Gaussian fits to the profiles, normalized by total counts). The gain loss at the aimpoint seems to be fairly linear with time - Figure 7 shows the medians as a function of time with a linear least-squares fit (dotted line) and a horizontal line (solid) for reference.

The evolution of the PHA response of the HRC-S at lower energies as witnessed by HZ 43 observations is currently being analyzed by the HRC-S/LETG calibration group. Various options for maintaining the performance of the HRC-S will be considered.

Figure 5: HRC-S AR Lac Observations: Median Source PHA

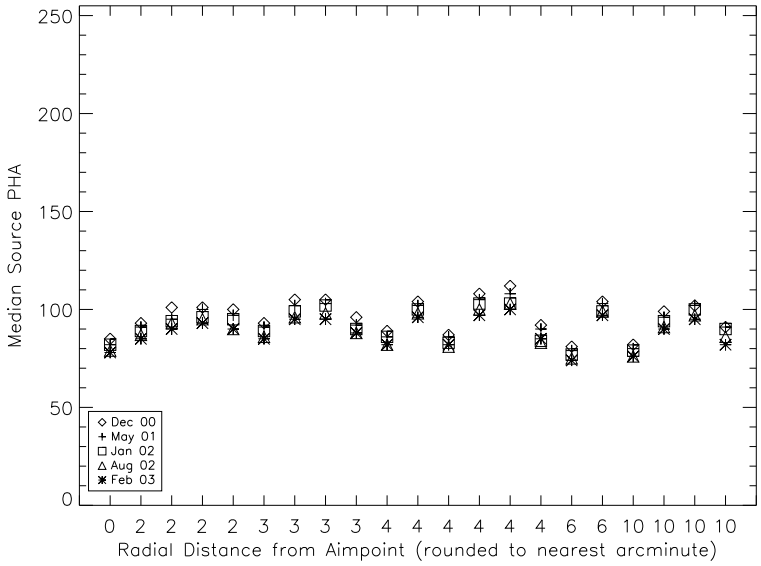

Figure 6: HRC-S AR Lac Observations: Gaussian Fits to PHA Distributions at Aimpoint

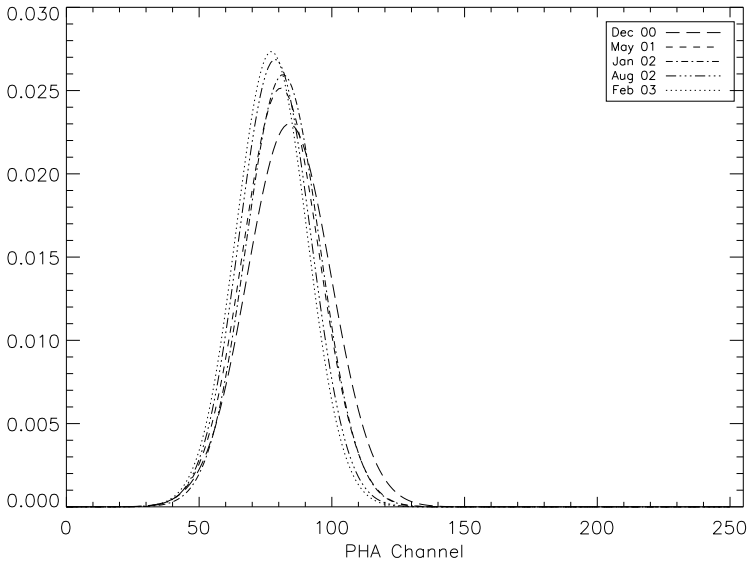

Figure 7: HRC-S AR Lac Observations: Median Source PHAs at Aimpoint

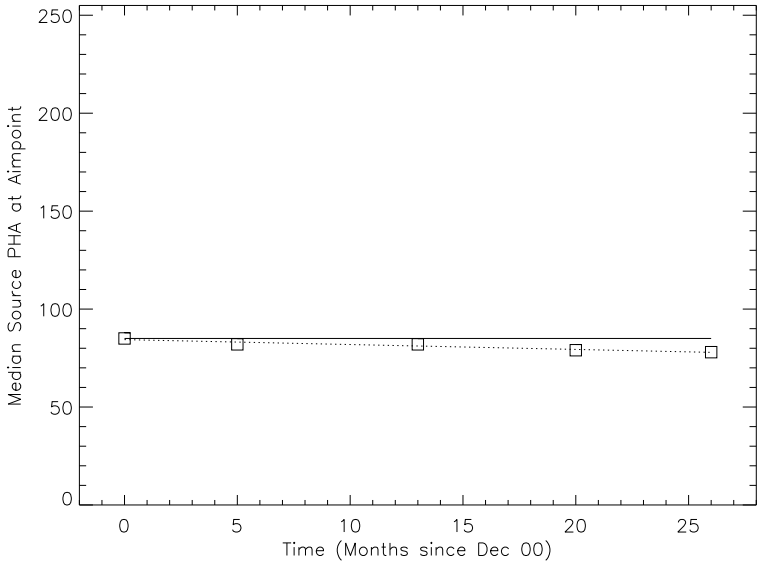

4 Summary

We analyze gain evolution in the HRC by comparing the source PHAs extracted from calibration observations of AR Lac taken over the past several years. For both detectors, we find that the median source PHAs at the aimpoint are migrating towards lower channels and that the PHA distributions are becoming more narrow. These trends are more dramatic in the HRC-I than in the HRC-S. Specifically, we find that since October 1999, the HRC-I has experienced a gain loss of roughly 19% at the aimpoint. (This gain loss is also seen at lower energies: analysis of the median source PHAs from HZ 43 observations taken over the past several years reveals a drop of about 16% at the aimpoint.) For the offset positions monitored on the HRC-I with AR Lac, the gain loss is smaller than at the aimpoint, decreasing from roughly 9% to 4% with radial distance from the aimpoint. For the HRC-S, we find a gain drop of 10% since December 2000, which is fairly uniform for all offset positions monitored.

Options for addressing the gain loss are being discussed. One possibility is that the voltage on the HRC-I will be adjusted to maintain the instrument's performance.

Appendix A

Table 1: Summary of HRC-I AR Lac Observations

Y offset	Z Offset	Radial Dist	Extraction Radius	Oct 99	Dec 99	Dec 00	Jan 02	Feb 03
arcmin	arcmin	arcmin	pixels	ObsID	ObsID	ObsID	ObsID	ObsID
0	0	0	60	1321	1484	0996	2608	4294
2	0	2	60	1324	1485	2345	2617	4303
0	2	2	60	1342	1491	2351	2611	4297
-2	0	2	60	1336	1489	2349	2610	4296
0	-2	2	60	1330	1487	2347	2618	4304
2	2	2.83	60	1345	1492	2352	2604	4290
-2	2	2.83	60	1339	1490	2350	2619	4305
-2	-2	2.83	60	1333	1488	2348	2624	4310
2	-2	2.83	60	1327	1486	2346	2609	4295
4	0	4	60	1348	1493	2353	2620	4306
0	4	4	60	1366	1499	2359	2606	4293
-4	0	4	60	1360	1497	2357	2621	4307
0	-4	4	60	1354	1495	2355	2612	4300
6	0	6	60	1351	1494	2354	2605	4291
0	6	6	60	1369	1500	2360	2607	4292
-6	0	6	60	1363	1498	2358	2613	4299
0	-6	6	60	1357	1496	2356	2614	4298
10	10	14.14	200	1372	1501	2361	2615	4301
-10	10	14.14	200	1381	1504	2364	2616	4302
-10	-10	14.14	200	1378	1503	2363	2623	4309
10	-10	14.14	200	1375	1502	2362	2622	4308

Table 2: Summary of HRC-S AR Lac Observations

Y offset	Z offset	Radial Dist	Extraction Radius	Dec 00	May 01	Jan 02	Aug 02	Feb 03
arcmin	arcmin	arcmin	pixels	ObsID	ObsID	ObsID	ObsID	ObsID
0	0	0	60	0998	0997	2629	2650	4336
2	0	2	60	2366	2432	2638	2659	4345
0	2	2	60	2372	2438	2632	2653	4339
-2	0	2	60	2370	2436	2631	2652	4338
0	-2	2	60	2368	2434	2639	2660	4346
2	2	2.83	60	2373	2439	2625	2646	4332
-2	2	2.83	60	2371	2437	2640	2661	4347
-2	-2	2.83	60	2369	2435	2645	2666	4352
2	-2	2.83	60	2367	2433	2630	2651	4337
4	0	4	60	2374	2440	2641	2662	4348
-4	0	4	60	2378	2444	2642	2663	4349
4	2	4.47	60	2381	2447	2627	2648	4334
-4	2	4.47	60	2380	2446	2635	2656	4342
-4	-2	4.47	60	2377	2443	2633	2654	4340
4	-2	4.47	60	2376	2442	2628	2649	4335
6	0	6	60	2375	2441	2626	2647	4333
-6	0	6	60	2379	2445	2634	2655	4341
10	2	10.20	200	2382	2448	2636	2657	4343
-10	2	10.20	200	2385	2451	2637	2658	4351
-10	-2	10.20	200	2384	2450	2644	2665	4344
10	-2	10.20	200	2383	2449	2643	2664	4350